


Article

The Pyla-1 Natural Accession of *Arabidopsis thaliana* Shows Little Nitrate-Induced Plasticity of Root Development

Silvana Porco ¹, Loïc Haelterman ¹, Jérôme De Pessemier ¹, Hugues De Gernier ^{1,2,3} , Florence Reyé ¹ and Christian Hermans ^{1,*} 

- ¹ Crop Production and Biostimulation Laboratory, Brussels Bioengineering School, Université Libre de Bruxelles, Campus Plaine CP 245, Bd du Triomphe, 1050 Brussels, Belgium
² Department of Plant Biotechnology and Bioinformatics, Ghent University, 9052 Ghent, Belgium
³ Center for Plant Systems Biology, VIB, Technologiepark 927, 9052 Ghent, Belgium
* Correspondence: christian.hermans@ulb.be; Tel.: +32-2-650-5416

Abstract: Optimizing root system architecture is a strategy for coping with soil fertility, such as low nitrogen input. An ample number of *Arabidopsis thaliana* natural accessions have set the foundation for studies on mechanisms that regulate root morphology. This report compares the Columbia-0 (Col-0) reference and Pyla-1 (Pyl-1) from a coastal zone in France, known for having the tallest sand dune in Europe. Seedlings were grown on vertical agar plates with different nitrate concentrations. The lateral root outgrowth of Col-0 was stimulated under mild depletion and repressed under nitrate enrichment. The Pyl-1 produced a long primary root and any or very few visible lateral roots across the nitrate supplies. This could reflect an adaptation to sandy soil conditions, where the primary root grows downwards to the lower strata to take up water and mobile soil resources without elongating the lateral roots. Microscopic observations revealed similar densities of lateral root primordia in both accessions. The Pyl-1 maintained the ability to initiate lateral root primordia. However, the post-initiation events seemed to be critical in modulating the lateral-root-less phenotype. In Pyl-1, the emergence of primordia through the primary root tissues was slowed, and newly formed lateral roots stayed stunted. In brief, Pyl-1 is a fascinating genotype for studying the nutritional influences on lateral root development.

Keywords: *Arabidopsis thaliana*; natural variation; nitrogen nutrition; root morphology



Citation: Porco, S.; Haelterman, L.; De Pessemier, J.; De Gernier, H.; Reyé, F.; Hermans, C. The Pyla-1 Natural Accession of *Arabidopsis thaliana* Shows Little Nitrate-Induced Plasticity of Root Development. *Nitrogen* **2022**, *3*, 444–454. <https://doi.org/10.3390/nitrogen3030029>

Academic Editor: Marouane Baslam

Received: 30 June 2022

Accepted: 6 August 2022

Published: 8 August 2022

Publisher's Note: MDPI stays neutral with regard to jurisdictional claims in published maps and institutional affiliations.



Copyright: © 2022 by the authors. Licensee MDPI, Basel, Switzerland. This article is an open access article distributed under the terms and conditions of the Creative Commons Attribution (CC BY) license (<https://creativecommons.org/licenses/by/4.0/>).

1. Introduction

Nitrogen (N) mineral fertilization is used to sustain crop production, but excessive concentrations of nitrate have harmful effects on the environment and human health by causing soil nitrate leaching, groundwater pollution and greenhouse gas emissions [1,2]. Improving decision tools for agricultural management and breeding crops for better nitrogen use efficiency (NUE) are implemented to reduce N fertilizer input [3–5]. The optimization of the root system architecture of crops for a more efficient N capture is a key determinant to reaching that goal. The root organ has plasticity to adapt to the nitrate supply: local nitrate patches stimulate lateral root outgrowth, whereas globally high external nitrate concentrations have a systemic inhibitory effect [6,7]. Increasing lateral root branching of a crop species would serve to explore a larger soil volume and to enhance nitrate capture [8–10].

In plant biology research, *Arabidopsis thaliana* has a long history of being used as a model for studying root organogenesis. The formation of a lateral root is a post-embryonic event that originates from the asymmetric division of the pericycle cell pair—a step referred to as the lateral root initiation [11–13]. The dividing pericycle cells develop into a lateral root primordium that emerges through the overlying tissues (subsequently, the endodermis, cortex and epidermis) of the parent root [14–16]. Next, the apical meristem is activated, and the newly formed lateral root elongates. Genetic screens have isolated a plethora

of *Arabidopsis* mutants with lateral root developmental defects [17]. Additionally, the *Arabidopsis* model represents a step forward in understanding the nitrate influences on root growth [18]. The variability of root morphologies, offered by abundant natural accessions, is exploited to mine for the genes and alleles that regulate root traits in response to the nitrate supply [19]. This knowledge may provide new targets to breed genetically related crops with larger genomes (e.g., cultivated *Brassica*), which could be more efficient at capturing N in the soil.

This study provides a detailed root phenotype characterization of Pyla-1 (Pyl-1), one natural *Arabidopsis* accession that is part of a core collection that maximizes the genetic diversity of the species [20]. The Pyl-1 originates from the coastal zone of Arcachon Bay in France, known for having the tallest sand dune in Europe. Following previous phenotyping screens conducted in vitro [21,22], the accession shows any or very few visible lateral roots at a young developmental stage. This report provides (i) a comparison of a two-dimensional root morphology between the Columbia-0 (Col-0) reference and Pyl-1 in response to a nitrate supply, and together with four accessions collected from the Arcachon urban area, (ii) a quantification of the total number and developmental stages of lateral root primordia, and (iii) a temporal sequence of the lateral root formation after a gravitropic curvature. These findings underline Pyl-1 as a prevailing genotype for studying the mechanisms of repression exerted by nitrate on lateral root growth.

2. Materials and Methods

2.1. Plant Material

The *Arabidopsis thaliana* Columbia-0 (Col-0) accession was obtained from the Nottingham *Arabidopsis* Stock Centre, and Pyla-1 (Pyl-1) was obtained from the INRAE Versailles Genomic Resource Center. The four Arcachon (Arc-1, Arc-2, Arc-3, Arc-4) accessions were collected in the Arcachon-Pyla area, France. The geographical map of the harvesting sites and coordinates is shown in Figure S1.

2.2. In Vitro Culture

The in vitro culture procedure is described in [22]. Briefly, sterilized seeds were plated on a 1× Murashige and Skoog medium, modified with nitrate as the only N source, 1% (*w/v*) sucrose and 0.8% (*w/v*) plant agar (Duscheff Biochemie, Haarlem, the Netherlands). The pH was adjusted to 5.7. Five media with different nitrate concentrations were prepared: 0.1 mM KNO₃ + 9.9 mM KCl (added to prevent potassium depletion), 1 mM KNO₃ + 9 mM KCl, 10 mM KNO₃, 25 mM KNO₃ or 50 mM KNO₃. A volume of 50 mL of medium was poured into one square Petri plate (12 cm × 12 cm). Five seeds of one genotype were sown on a Petri plate and were stratified for two days at 4 °C in the dark. The plates were vertically incubated in a culture chamber with a constant temperature of 20 °C and a photoperiod of 16 h light (45 μmol photons m⁻² s⁻¹) / 8 h darkness.

2.3. Two-Dimensional Root Morphology Analysis

Eleven days after germination, the root systems were scanned with an EPSON Scan Perfection V30 at a resolution of 400 dpi. The scans were annotated using the RootNav image analysis software [23]. The length of the primary root (L_{PR}), the number of lateral roots that visibly emerged from the primary root longer than 1 mm (N_{LR}) and the sum of the length of lateral roots (ΣL_{LR}) were quantified [22].

2.4. Quantification of Lateral Root Primordium Developmental Stages

The roots were cleared following the protocol detailed in [24]. The developmental stages of lateral root primordia were observed with an Optika B-350 microscope. Nine categories were established: I (initiating primordium), II–III (up to three cell layers structure), IV–VII (primordium dome formation and emergence through parental tissues), E (lateral root emerged from the epidermis and of less than 1 mm) and LR (lateral root strictly longer

than 1 mm). The total number of lateral root primordia (N_{LRP}) and the density of lateral root primordia per primary root length (D_{LRP}) were measured 11 days after germination.

2.5. Lateral Root Bending

The seeds were plated on a medium containing 10 mM KNO_3 . The seedlings were grown for three days under continuous light ($45 \mu\text{mol photons m}^{-2} \text{s}^{-1}$) conditions. The plates positioned vertically were turned 90° , as described in [25]. The roots were collected at eight different time points (18 h, 24 h, 30 h, 36 h, 42 h, 48 h, 54 h and 60 h) after rotation. The root bends were cleared (see Section 2.4), and the development stages of the lateral root primordia (from initiation to emergence) were scored.

2.6. Statistical Treatment

All statistical analyses were done with R software [26] and XLSTAT [27]. An analysis of variance was performed for the variables L_{PR} , N_{LR} , ΣL_{LR} , N_{LRP} and D_{LRP} , using the lme4 R package [28]. The phenotypic models were fitted on the Col-0 and Pyl-1 genotypes using the REML method, according to the equation $P_{ijk} = \mu + G_i + N_j + G_i \times N_j + e_{ijk}$, where P_{ijk} is the phenotypic value, μ is the general mean, G_i is the genotype i , N_j is the nitrate supply j , and e_{ijk} is the residual. All effects were declared as random. Moreover, multiple t -tests were performed using the tidyverse and rstatix R packages [29,30] to compare the mean values of the root morphological traits under each genotype \times nitrate combination.

3. Results

3.1. The Pyla-1 Accession Exhibited Little Macroscopic Variation of Root Morphology in Response to Nitrate Supply

The seedlings of Col-0 and Pyl-1 grew vertically on media supplemented with 0.1, 1, 10, 25 or 50 mM nitrate. The morphological variation of the whole root organs is shown in Figure 1. The length of the primary root (L_{PR}), the number of visible lateral roots > 1 mm (N_{LR}) and the sum of the length of lateral roots (ΣL_{LR}) reached the greatest values in the Col-0 seedlings supplied with 1 mM nitrate (Figure 2). The modulation of the root morphology by nitrate availability followed the previous observations in the reference accession [31,32]. A low but moderate nitrate supply (1 mM) promoted the growth of both the primary and lateral roots, while a severe nitrate shortage (0.1 mM) and elevated nitrate supply (>25 mM) repressed the number and the length of lateral roots in Col-0 (Figure 2). By contrast, Pyl-1 was slightly responsive to the nitrate supply and produced very few short lateral roots, solely at 0.1 mM nitrate. For every nitrate concentration tested, the L_{PR} values were significantly ($p < 0.05$) greater in Pyl-1 than in Col-0, while N_{LR} and ΣL_{LR} were lower (Figure 2). We assessed the extent to which a variation in the root morphological traits was due to the genetic differences between accessions (G), nitrate treatment differences (N), genetic differences in the level of response to nitrate treatment ($G \times N$) and unexplained experimental errors (residuals) (Figure S2). Most of the variations for L_{PR} and N_{LR} were due to G (35% and 65%, respectively). The ΣL_{LR} trait showed a nearly equal dependence on G (47%) and $G \times N$ (44%). This highlighted a larger genotype-dependent plasticity to the nitrate treatment for ΣL_{LR} than for L_{PR} or N_{LR} .

All four Arcachon accessions showed similar root morphologies at 10 mM nitrate (Figure 1). The L_{PR} , N_{LR} and ΣL_{LR} values were significantly ($p < 0.05$) lower compared to Col-0 (Figure 2). Only L_{PR} was identical between Arc-4 and Col-0. Contrastingly, these accessions did not mimic the Pyl-1 root phenotype; rather, they presented shorter L_{PR} and more important N_{LR} and ΣL_{LR} values than Pyl-1.

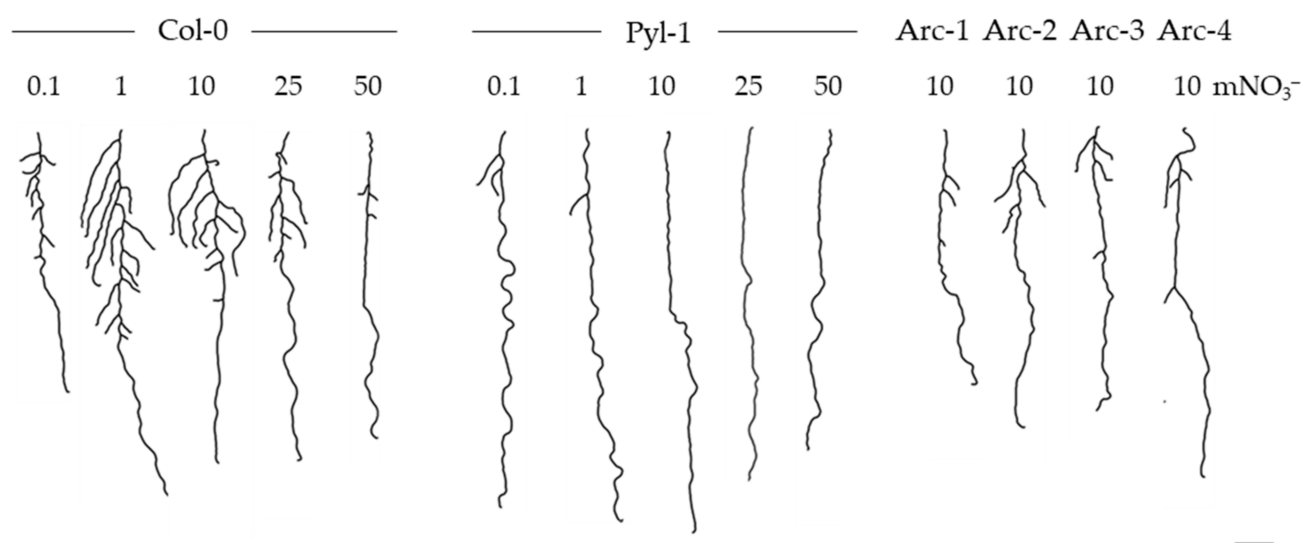


Figure 1. Root phenotypes of Arabidopsis accessions in response to nitrate supply. Pyl-1 (Pyl-1), Columbia-0 (Col-0) accessions are germinated on media containing 0.1, 1, 10, 25 or 50 mM nitrate and Arcachon accessions (Arc-1, Arc-2, Arc-3, Arc-4) on 10 mM nitrate. Pictures were taken 11 days after germination. Scale bar: 1 cm.

3.2. The Initiation of Lateral Root Primordium Was Not Impaired in Pyl-1

One possible explanation for the lateral-root-less phenotype harbored by Pyl-1 (Figure 1) could be an impairment of lateral root initiation. Hence, we examined the lateral root development at the microscopic level (Figure 3). In both genotypes, the number of lateral root primordia (N_{LRP}) globally decreased with the nitrate concentration increasing. The N_{LRP} was significantly ($p < 0.05$) more important in Pyl-1 compared to Col-0 at 0.1, 1 and 50 mM nitrate (Figure 3a). No significant difference in the density of lateral root primordia (D_{LRP}) was observed between the genotypes across all nitrate concentrations; however, D_{LRP} was greater in Pyl-1 than Col-0 at 50 mM nitrate (Figure 3b). By contrast, with the macroscopic root morphological traits (Figure 2), N_{LRP} and D_{LRP} showed a large N treatment effect (44% and 71%, respectively) (Figure S2).

The lateral root formation follows a precise developmental program during which successive phases, from the initiation to the emergence, arise to penetrate the parent root tissue layers [33] (Figure 3c). At 1 mM nitrate, almost three-quarters of the lateral root primordia emerged from the primary root in Col-0 (Figure 3d). That proportion decreased when the seedlings were subjected to lower or greater nitrate concentrations. The percentages of the emerged (<1 mm) and visible (>1 mm) lateral roots were 54 % and 13%, respectively, at 0.1 mM nitrate, while these values reached 28% and 33% at 50 mM nitrate. By comparison, three-thirds of the Pyl-1 primordia had not emerged from the primary root at 1 mM nitrate. The percentages of the emerged and visible lateral roots reached 23% and 19%, respectively, at 0.1 mM nitrate, while only 7% emerged at 50 mM nitrate. Across all nitrate concentrations, Pyl-1 had greater cumulated percentages at stages III, IV and V compared to Col-0 (Figure 3d). At 50 mM nitrate, more than one-third of the primordia stayed at stage IV. This indicates that the intermediate stages of progression through the cortex tissue were affected rather than at the initiation.

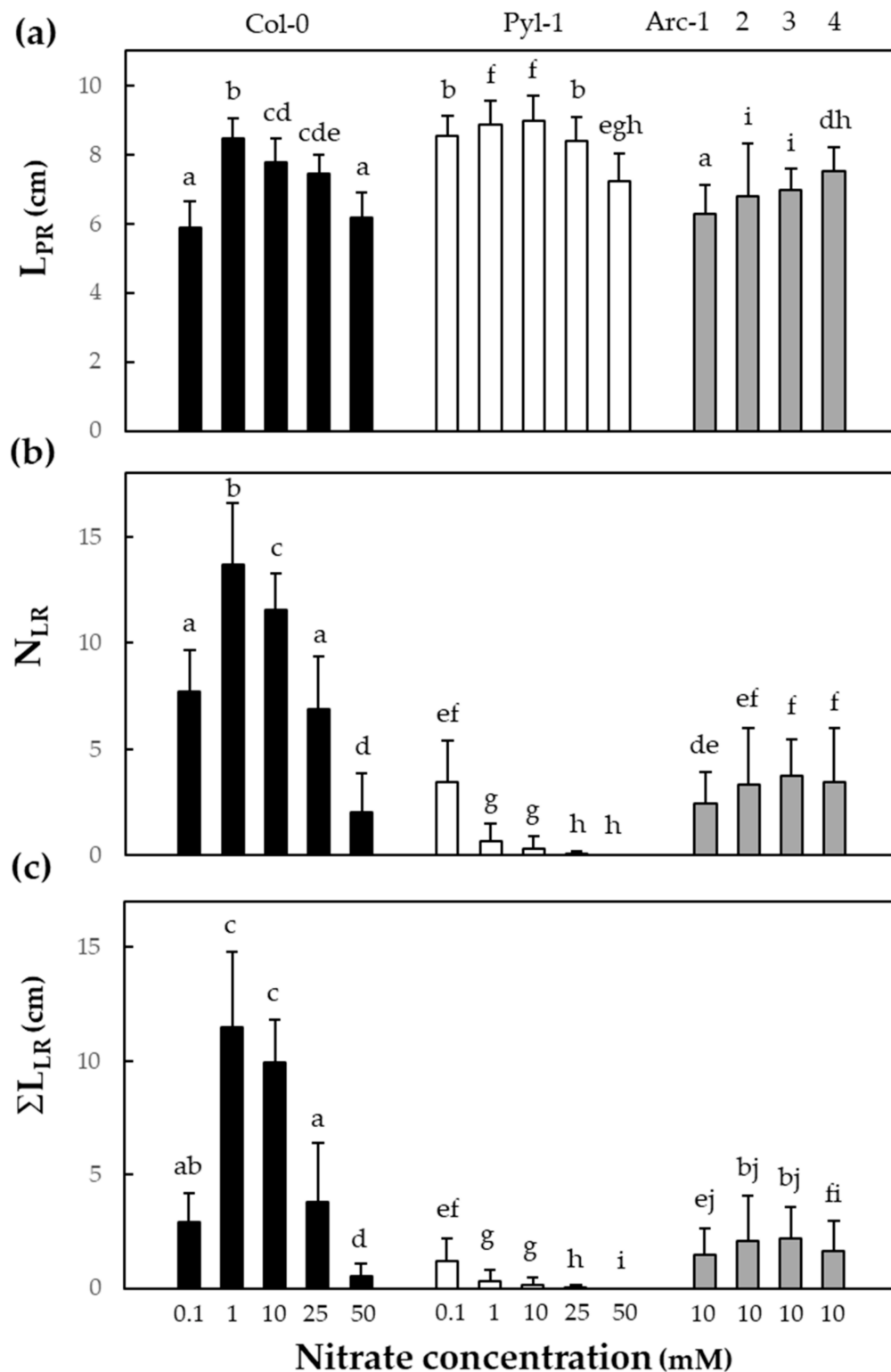


Figure 2. Root morphological traits of Columbia-0, Pyla-1 and Arcachon accessions in response to nitrate supply. Plants were grown as described in the legend of Figure 1. (a) Length of the primary root (L_{PR}); (b) number of lateral roots longer than 1 mm length (N_{LR}); (c) sum of the length of lateral roots (ΣL_{LR}). Black columns: Col-0, white columns: Pyl-1, gray columns: Arc-1, Arc-2, Arc-3 and Arc-4. $n = 20\text{--}48$ root organs \pm std. Data are analyzed with multiple t -tests, and the different letters allow for visualizing the significant differences. Values sharing the same letter are not significantly different (p -value > 0.05). Phenotypic models are shown in Table S1.

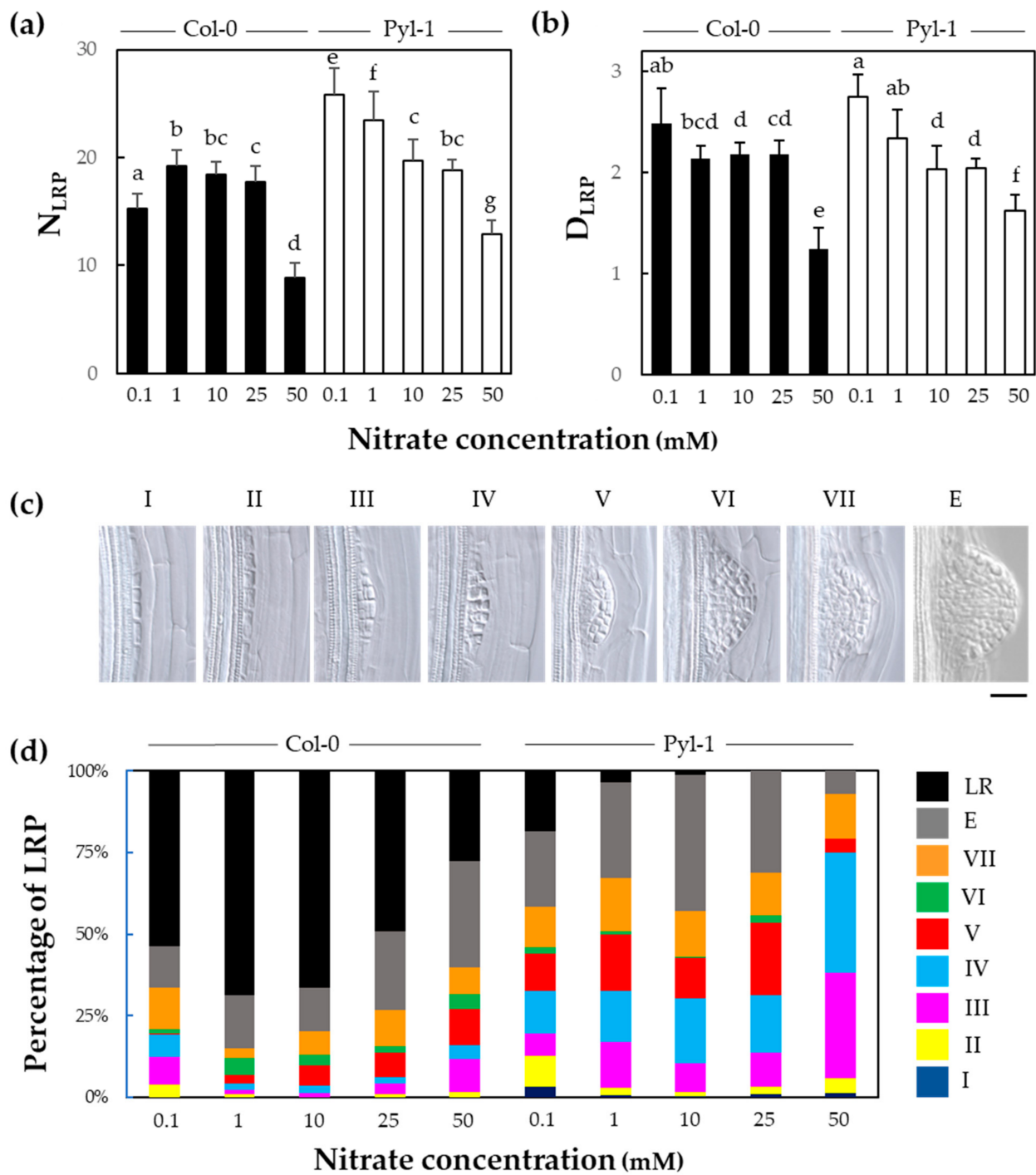


Figure 3. Lateral root primordium quantification of Pyl-1 and Columbia-0 accessions in response to nitrate supply. The total number of lateral root primordia (N_{LRP}) (a) and the density of lateral root primordia (D_{LRP}) (b) were measured under 0.1, 1, 10, 25 and 50 mM nitrate supplies 11 days after germination. Growth conditions are described in Figure 1. Black columns: Col-0, white columns: Pyl-1. $n = 12$ observations \pm std. Data are analyzed with multiple t -tests, and the different letters allow for visualizing the significant differences. Values sharing the same letter are not significantly different (p -value > 0.05). (c) Microscopic pictures illustrate nine stages of lateral root primordium development in Col-0, indicated by Roman numbers I–VII (initiation to emergence through parental tissues) and E (primordium emerged from the epidermis). Scale bar: 20 μ m. (d) The distribution of lateral root primordia (LRP) between developmental stages I–VIII, E and LR (mature lateral root of strictly more than 1 mm). $n = 12$ observations.

3.3. Lateral Root Primordia Exhibit Slower Organ Emergence in Pyl-1

A root bending assay was conducted to follow the temporal sequence of lateral root formation. By applying a 90° gravitropic stimulus, the lateral root initiation was synchronically induced at the outer edges of the bending roots. Then, the developmental stages of the lateral root primordia at the root bends were scored every 6 h between 18 h and until their emergence from the primary root. In Col-0, the lateral root initiation (stage I) was detected 18 h post gravity induction, and the emergence (stage E) happened after 42 h (Figure 4a). These observations matched with previous reports on the reference accession [25]. In Pyl-1, the lateral root initiation happened at the same time compared to Col-0. However, stages I and II accumulated during the first hours, and the progression to stages III and IV was drastically delayed (Figure 4b). After 42 h, most Pyl-1 primordia were still blocked around these stages. Eventually, the primordia progressed to the later stages, VI and VII, with the majority of them emerging from the parent root after 60 h. The newly emerged lateral roots did not elongate after that time (data not shown). These data indicated that Pyl-1 had a slower lateral root developmental program with a bottleneck around stages III–V. The accumulation of these specific stages pointed to a defect in the transition from a flat to dome-shaped lateral root primordium [15,34]. This prompted us to examine the shapes of primordia (length, height and area) at stages II, III and IV in the two genotypes (Figure S2). The length and/or the area of the primordia were significantly ($p < 0.05$) increased by 5–15% in Pyl-1 compared to Col-0. This is documenting that the Pyl-1 lateral root primordium is misshaped.

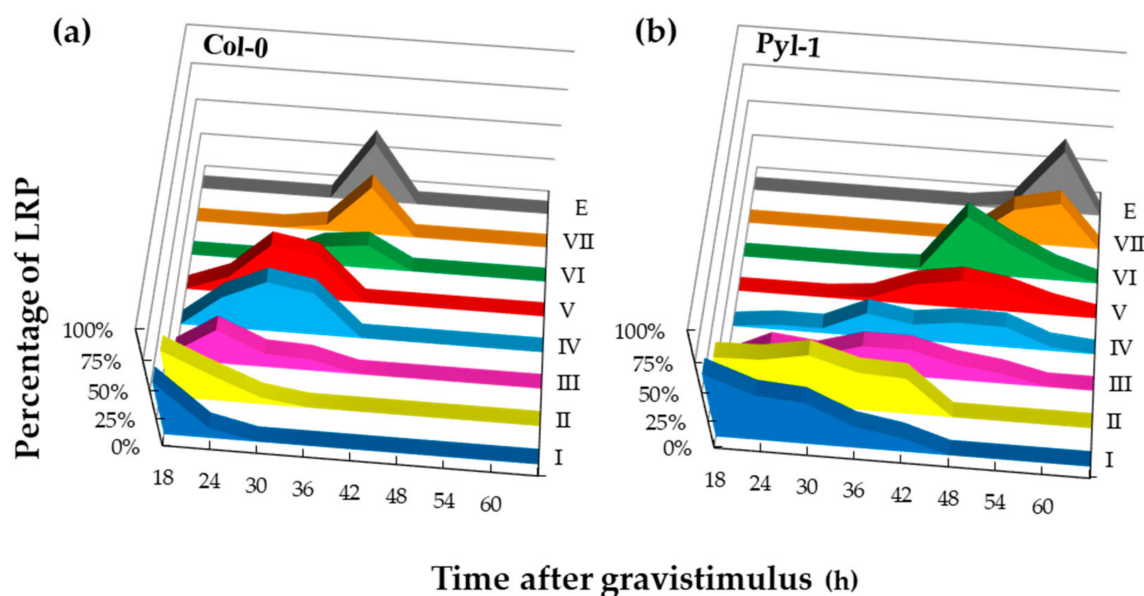


Figure 4. Time course of lateral root primordium development in Columbia-0 and Pyl-1 accessions. Developmental stages (from I to VIII) were determined every 6 h post-stimulus and were represented as a percentage of the total number of induced lateral root primordia (LRP) in Col-0 (a) and Pyl-1 (b). Bending assays were conducted on media containing 10 mM nitrate. $n = 25$ –30 observations.

4. Discussion

The *Arabidopsis thaliana* species has a vast geographical distribution. Natural populations growing in a wide range of soil conditions around the world are showing a large variation in the expression of numerous phenotypic traits and also at the root organ level [35,36]. These accessions provide a rich and diverse genetic resource for studying NUE processes [37–40] and the N-related adaptive differences in root morphology [41,42]. The Pyl-1 accession shows a fascinating root phenotype that is slightly responsive to nitrate availability (Figure 1).

The developmental and morphological defects are largely documented during the lateral root organogenesis of the *Arabidopsis* model [17,43]. For instance, the *alf4-1*, *arf7arf19*, *gata23*, and *slr-1* mutants [44–47] are unable to trigger the initiation cascade, resulting in a lateral-root-less phenotype. In terms of the macroscopic root architecture, Pyl-1 looks very similar to these mutants. However, this natural accession has identical or even greater densities of lateral root primordia compared to the Col-0 wild-type (Figure 3a). This clearly indicates that Pyl-1 maintains the ability to initiate lateral root primordia. Thus, the post-initiation events seem to be critical in modulating the Pyl-1 macroscopic root morphology. A biomechanical constraint may be exerted on the primordia breaking through overlying tissues. Such a mechanical constraint is documented to cause a change in primordium shape [14,17]. The contours of some Pyl-1 primordia are altered (Figure S2), further pointing to such mechanical properties of the cortex. Further studies on the tensile properties of tissues need to be carried out.

During the lateral root formation sequence (Figure 3d), the progression occurring from early primordium development is slowed down, with a bottleneck arising around stages III–V, followed by a later constraint on the elongation out of the parent root. These defects likely involve the phytohormone auxin, which is a key regulator of lateral root formation [48]. The auxin accumulation in the cells overlying the primordium depends on transcription factor LATERAL ORGAN BOUNDARIES-DOMAIN 29 (LBD29) regulating the auxin influx carrier LIKE-AUX1 3 (LAX3) [15,49]. The loss-of-function of these two genes results in a slowdown from stages III to V [15,49], as observed in Pyl-1. Moreover, this hormone alters cell wall properties by inducing wall loosening [50], and auxin-dependent cell separation promotes lateral organ emergence [15]. Furthermore, auxin regulates the root tissue hydraulic properties and aquaporin function to facilitate emergence [25]. Altering PLASMA MEMBRANE INTRINSIC PROTEIN 2;1 (PIP2;1) causes a flattened dome-shape primordia and delays emergence [25]. Another case was reported on the overexpression of MYB DOMAIN PROTEIN 93 (MYB93) negatively impacting the primordium progression [51,52]. Likewise, the loss of the MYB36 function results in the accumulation of stages IV–V [34]. A thorough analysis of the genetic and developmental background of the Pyl-1 root phenotype will be essential in the future.

The natural *Arabidopsis* populations undergo various selective environmental pressures. Developmental and physiological adaptations are likely to occur in order to optimize plant performance in different habitats [53,54]. The Pyl-1 accession was initially collected in the Pyla area, Arcachon Bay, France. There, the tallest sand dune in Europe is found. The Pyl-1 root phenotype observed *in vitro* (Figure 1) may reflect an adaptation to sandy soil conditions, where the primary root grows downwards to the lower strata to take up water without elongating the lateral roots. However, the lack of data on local soil conditions makes it difficult to support this hypothesis further. Therefore, we launched a prospection campaign in the Arcachon Bay area. No accession was found in the Dune of Pilat, but four of them were collected in the Arcachon urban environment (Figure S1). These accessions were growing on sidewalks in the city, and soil sampling was impossible. Thus, the hypothesis of an adaptation to a sand habitat is still lacking to support field evidence at this stage. Additional observations of root morphology upon growth conditions in rhizotrons filled with sand could provide more indications of the Pyl-1 phenotype.

5. Conclusions

Pyl-1 is a fascinating plant material for studying root organogenesis. The next step will be to identify the allele(s) responsible for the lateral-root-less phenotype. After generating one F2 (Col-0 × Pyl-1)-segregating population, a mapping-by-sequencing strategy [55] could be employed on two pooled genomes showing contrasting lateral root outgrowth. A further molecular characterization could involve monitoring the expression of the genes involved in cell separation and lateral root emergence. The molecular dissection of the lateral root development in Pyl-1 could greatly contribute to drawing strategies for optimizing the root system architecture and improving N capture in plants.

Supplementary Materials: The following are available online at <https://www.mdpi.com/article/10.3390/nitrogen3030029/s1>, Table S1: Variance components extracted from mixed linear models, Figure S1: Arabidopsis accessions in the Arcachon Bay area, France, Figure S2: Comparison of the shape of lateral root primordia in Columbia-0 and Pyla-1 accessions.

Author Contributions: Conceptualization: C.H.; Original draft preparation: C.H. and S.P.; Investigation, methodology: C.H., F.R., J.D.P., H.D.G. and L.H. All authors have read and agreed to the published version of the manuscript.

Funding: This research was funded by Fonds de la Recherche Scientifique (F.R.S.-FNRS) (MIS and CDR J.0106.20).

Institutional Review Board Statement: Not applicable.

Informed Consent Statement: Not applicable.

Data Availability Statement: The data presented in this study are available on request from the corresponding author.

Acknowledgments: L.H. and C.H. are, respectively, a PhD fellow and research associate from F.R.S.-FNRS.

Conflicts of Interest: The authors declare no conflict of interest.

References

1. Walling, E.; Vaneekhaute, C.J. Greenhouse gas emissions from inorganic and organic fertilizer production and use: A review of emission factors and their variability. *J. Environ. Manage.* **2020**, *276*, 111211. [CrossRef]
2. Picetti, R.; Deeney, M.; Pastorino, S.; Miller, M.R.; Shah, A.; Leon, D.A.; Dangour, A.D.; Green, R. Nitrate and nitrite contamination in drinking water and cancer risk: A systematic review with meta-analysis. *Environ. Res.* **2022**, *210*, 112988. [CrossRef]
3. Lebedev, V.G.; Popova, A.A.; Shestibratov, K.A. Genetic engineering and genome editing for improving nitrogen use efficiency in plants. *Cells* **2021**, *10*, 3303. [CrossRef]
4. Javed, T.; Indu, I.; Singhal, R.K.; Shabbir, R.; Shah, A.N.; Kumar, P.; Jinger, D.; Dharmappa, P.M.; Shad, M.A.; Saha, D.; et al. Recent advances in agronomic and physio-molecular approaches for improving nitrogen use efficiency in crop plants. *Front. Plant. Sci.* **2022**, *13*, 877544. [CrossRef]
5. Whetton, R.L.; Harty, M.A.; Holden, N.M. Communicating nitrogen loss mechanisms for improving nitrogen use efficiency management, focused on global wheat. *Nitrogen* **2022**, *3*, 213–246. [CrossRef]
6. Walch-Liu, P.; Ivanov, I.I.; Filleur, S.; Gan, Y.; Remans, T.; Forde, B.G. Nitrogen regulation of root branching. *Ann. Bot.* **2006**, *97*, 875–881. [CrossRef]
7. Asim, M.; Ullah, Z.; Xu, F.; An, L.; Aluko, O.O.; Wang, Q.; Liu, H. Nitrate signaling, functions, and regulation of root system architecture: Insights from *Arabidopsis thaliana*. *Genes* **2020**, *11*, 633. [CrossRef]
8. Louvieaux, J.; Spanoghe, M.; Hermans, C. Root morphological traits of seedlings are predictors of seed yield and quality in winter oilseed rape hybrid cultivars. *Front. Plant. Sci.* **2020**, *11*, 568009. [CrossRef]
9. Kupcsik, L.; Chiodi, C.; Moturu, T.R.; De Gernier, H.; Haelterman, L.; Louvieaux, J.; Tillard, P.; Sturrock, C.J.; Bennett, M.; Nacry, P.; et al. Oilseed rape cultivars show diversity of root morphologies with the potential for better capture of nitrogen. *Nitrogen* **2021**, *2*, 491–505. [CrossRef]
10. Wang, H.; Wu, Y.; An, T.; Chen, Y.J. Lateral root elongation enhances nitrogen-use efficiency in maize genotypes at the seedling stage. *J. Sci. Food Agric.* **2022**. [CrossRef]
11. Casimiro, I.; Marchant, A.; Bhalerao, R.; Beeckman, T.; Dhooge, S.; Swarup, R.; Graham, N.; Inzé, D.; Sandber, G.; Casero, P.; et al. Auxin transport promotes Arabidopsis lateral root initiation. *Plant. Cell* **2001**, *13*, 843–852. [CrossRef]
12. Dubrovsky, J.G.; Rost, T.L.; Colón-Carmona, A.; Doerner, P. Early primordium morphogenesis during lateral root initiation in *Arabidopsis thaliana*. *Planta* **2001**, *214*, 30–36. [CrossRef]
13. Du, Y.; Scheres, B. Lateral root formation and the multiple roles of auxin. *J. Exp. Bot.* **2018**, *69*, 155–167. [CrossRef]
14. Lucas, M.; Kenobi, K.; von Wangenheim, D.; Voß, U.; Swarup, K.; De Smet, I.; Van Damme, D.; Lawrence, T.; Péret, B.; Moscardi, E.; et al. Lateral root morphogenesis is dependent on the mechanical properties of the overlaying tissues. *Proc. Natl. Acad. Sci. USA* **2013**, *110*, 5229–5234. [CrossRef]
15. Porco, S.; Larrieu, A.; Du, Y.; Gaudinier, A.; Goh, T.; Swarup, K.; Swarup, R.; Kuempers, B.; Bishopp, A.; Lavenus, J.; et al. Lateral root emergence in Arabidopsis is dependent on transcription factor LBD₂₉ regulation of auxin influx carrier LAX₃. *Development* **2016**, *143*, 3340–3349.
16. Malamy, J.E.; Benfey, P.N. Down and out in Arabidopsis: The formation of lateral roots. *Trends Plant. Sci.* **1997**, *2*, 390–396. [CrossRef]
17. Szymanowska-Pulka, J. Form matters: Morphological aspects of lateral root development. *Ann. Bot.* **2013**, *112*, 1643–1654. [CrossRef]

18. Fredes, I.; Moreno, S.; Díaz, F.P.; Gutiérrez, R.A. Nitrate signaling and the control of Arabidopsis growth and development. *Curr. Opin. Plant. Biol.* **2019**, *47*, 112–118. [\[CrossRef\]](#)
19. Péliissier, P.-M.; Motte, M.; Beeckman, T. Lateral root formation and nutrients: Nitrogen in the spotlight. *Plant. Physiol.* **2021**, *187*, 1104–1116. [\[CrossRef\]](#)
20. McKhann, H.I.; Camilleri, C.; Bérard, A.; Bataillon, T.; David, J.L.; Reboud, X.; Le Corre, V.; Caloustian, C.; Gut, I.G.; Brunel, D. Nested core collections maximizing genetic diversity in Arabidopsis thaliana. *Plant. J.* **2004**, *38*, 193–202. [\[CrossRef\]](#)
21. De Pessemier, J.; Chardon, F.; Juraniec, M.; Delaplace, P.; Hermans, C. Natural variation of the root morphological response to nitrate supply in Arabidopsis thaliana. *Mech. Dev.* **2013**, *130*, 45–53. [\[CrossRef\]](#)
22. De Pessemier, J.; Moturu, T.R.; Nacry, P.; Ebert, R.; De Gernier, H.; Tillard, P.; Swarup, K.; Wells, D.M.; Haseloff, J.; Murray, S.C.; et al. Root system size and root hair length are key phenes for nitrate acquisition and biomass production across natural variation in Arabidopsis. *J. Exp. Bot.* **2022**, *73*, 3569–3583. [\[CrossRef\]](#)
23. Pound, M.P.; French, A.P.; Atkinson, J.A.; Wells, D.M.; Bennett, M.J.; Pridmore, T. RootNav: Navigating images of complex root architectures. *Plant. Physiol.* **2013**, *162*, 1802–1814. [\[CrossRef\]](#)
24. Dubrovsky, J.G.; Gambetta, G.A.; Hernández-Barrera, A.; Shishkova, S.; González, I. Lateral root initiation in Arabidopsis: Developmental window, spatial patterning, density and predictability. *Ann. Bot.* **2006**, *97*, 903–915. [\[CrossRef\]](#)
25. Péret, B.; Li, G.; Zhao, J.; Band, L.R.; Voß, U.; Postaire, O.; Luu, D.-T.; Da Ines, O.; Casimiro, I.; Lucas, M.; et al. Auxin regulates aquaporin function to facilitate lateral root emergence. *Nature Cell Biol.* **2012**, *14*, 991–998. [\[CrossRef\]](#)
26. R Core Team. *R: A Language and Environment for Statistical Computing*; R Foundation for Statistical Computing: Vienna, Austria, 2020; Available online: <https://www.R-project.org/> (accessed on 30 June 2022).
27. XLSTAT. Statistical Software for Excel. 2007. Available online: <https://www.xlstat.com> (accessed on 30 June 2022).
28. Bates, D.; Mächler, M.; Bolker, B.; Walker, S. Fitting linear mixed-effects models using lme4. *J. Stat. Softw.* **2015**, *67*, 1–48. [\[CrossRef\]](#)
29. Wickham, H.; Averick, M.; Bryan, J.; Chang, W.; McGowan, L.; François, R.; Grolemund, G.; Hayes, A.; Henry, L.; Hester, J.; et al. Welcome to the Tidyverse. *JOSS* **2019**, *4*, 1686. [\[CrossRef\]](#)
30. Kassambara, A. Rstatix: Pipe-Friendly Framework for Basic Statistical Tests. R Package Version 0.7.0. 2021. Available online: <https://rpkgs.datanovia.com/rstatix/> (accessed on 30 June 2022).
31. Sun, C.H.; Yu, Q.; Hu, D.G. Nitrate: A crucial signal during lateral roots development. *Front. Plant. Sci.* **2017**, *8*, 485. [\[CrossRef\]](#)
32. Louvieaux, J.; De Gernier, H.; Hermans, C. Exploiting genetic variability of root morphology as a lever to improve nitrogen use efficiency in oilseed rape. In *Engineering Nitrogen Utilization in Crop Plants*; Springer: Berlin/Heidelberg, Germany, 2018; pp. 185–201.
33. Malamy, J.E.; Benfey, P.N. Organization and cell differentiation in lateral roots of Arabidopsis thaliana. *Development* **1997**, *124*, 33–44. [\[CrossRef\]](#)
34. Fernández-Marcos, M.; Desvoves, B.; Manzano, C.; Liberman, L.M.; Benfey, P.N.; Del Pozo, J.C.; Gutierrez, C. Control of Arabidopsis lateral root primordium boundaries by MYB36. *New Phytol.* **2017**, *213*, 105–112. [\[CrossRef\]](#)
35. Deja-Muyllé, A.; Parizot, B.; Motte, H.; Beeckman, T. Exploiting natural variation in root system architecture via genome-wide association studies. *J. Exp. Bot.* **2020**, *71*, 2379–2389. [\[CrossRef\]](#)
36. Deja-Muyllé, A.; Opdenacker, D.; Parizot, B.; Motte, H.; Lobe, G.; Storme, V.; Clauw, P.; Njo, M.; Beeckman, T. Genetic variability of Arabidopsis thaliana mature root system architecture and genome-wide association study. *Front. Plant. Sci.* **2022**, *12*, 814110. [\[CrossRef\]](#)
37. North, K.A.; Ehrling, B.; Koprivova, A.; Rennenberg, H.; Kopriva, S. Natural variation in Arabidopsis adaptation to growth at low nitrogen conditions. *Plant. Physiol. Biochem.* **2009**, *47*, 912–918. [\[CrossRef\]](#)
38. Chardon, F.; Barthélémy, J.; Daniel-Vedele, F.; Masclaux-Daubresse, C. Natural variation of nitrate uptake and nitrogen use efficiency in Arabidopsis thaliana cultivated with limiting and ample nitrogen supply. *J. Exp. Bot.* **2010**, *61*, 2293–2302. [\[CrossRef\]](#) [\[PubMed\]](#)
39. Masclaux-Daubresse, C.; Chardon, F. Exploring nitrogen remobilization for seed filling using natural variation in Arabidopsis thaliana. *J. Exp. Bot.* **2011**, *62*, 2131–2142. [\[CrossRef\]](#)
40. Meyer, R.C.; Gryczka, C.; Neitsch, C.; Müller, M.; Bräutigam, A.; Schlereth, A.; Schön, H.; Weigelt-Fischer, K.; Altmann, T. Genetic diversity for nitrogen use efficiency in Arabidopsis thaliana. *Planta* **2019**, *250*, 41–57. [\[CrossRef\]](#)
41. Gifford, M.L.; Banta, J.A.; Katari, M.S.; Hulsmans, J.; Chen, L.; Ristova, D.; Tranchina, D.; Purugganan, M.D.; Coruzzi, G.M.; Birnbaum, K.D. Plasticity regulators modulate specific root traits in discrete nitrogen environments. *PLoS Genet.* **2013**, *9*, e1003760. [\[CrossRef\]](#)
42. Jia, Z.; Giehl, R.F.H.; von Wirén, N. The root foraging response under low nitrogen depends on DWARF1-mediated brassinosteroid biosynthesis. *Plant. Physiol.* **2020**, *183*, 998–1010. [\[CrossRef\]](#)
43. Sathbai, S.B.; Ristova, D.; Busch, W. Underground tuning: Quantitative regulation of root growth. *J. Exp. Bot.* **2015**, *66*, 1099–1112. [\[CrossRef\]](#)
44. Celenza Jr., J. L.; Grisafi, P.L.; Fink, G.R. A pathway for lateral root formation in Arabidopsis thaliana. *Genes Dev.* **1995**, *9*, 2131–2142. [\[CrossRef\]](#)
45. Okushima, Y.; Fukaki, H.; Onoda, M.; Theologis, A.; Tasaka, M. ARF7 and ARF19 regulate lateral root formation via direct activation of LBD/ASL genes in Arabidopsis. *Plant Cell.* **2007**, *19*, 118–130. [\[CrossRef\]](#) [\[PubMed\]](#)

46. De Rybel, B.; Vassileva, V.; Parizot, B.; Demeulenaere, M.; Grunewald, W.; Audenaert, D.; Van Campenhout, J.; Overvoorde, P.; Jansen, L.; Vanneste, S.; et al. A novel aux/IAA₂₈ signaling cascade activates GATA₂₃-dependent specification of lateral root founder cell identity. *Curr. Biol.* **2010**, *20*, 697–706. [[CrossRef](#)]
47. Fukaki, H.; Tameda, S.; Masuda, H.; Tasaka, M. Lateral root formation is blocked by a gain-of-function mutation in the *SOLITARY-ROOT/IAA14* gene of *Arabidopsis*. *Plant. J.* **2022**, *29*, 153–168. [[CrossRef](#)]
48. Lavenus, J.; Goh, T.; Roberts, I.; Guyomarc'h, S.; Lucas, M.; De Smet, I.; Fukaki, H.; Beeckman, T.; Bennett, M.; Laplace, L. Lateral root development in *Arabidopsis*: Fifty shades of auxin. *Trends Plant. Sci.* **2013**, *18*, 450–458. [[CrossRef](#)]
49. Swarup, K.; Benková, E.; Swarup, R.; Casimiro, I.; Péret, B.; Yang, Y.; Parry, G.; Nielsen, E.; De Smet, I.; Vanneste, S.; et al. The auxin influx carrier LAX3 promotes lateral root emergence. *Nat. Cell Biol.* **2008**, *10*, 946–954. [[CrossRef](#)] [[PubMed](#)]
50. Majda, M.; Robert, S. The role of auxin in cell wall expansion. *Int. J. Mol. Sci.* **2018**, *19*, 951. [[CrossRef](#)] [[PubMed](#)]
51. Gibbs, D.; Voss, U.; Harding, S.; Fannon, J.; Moody, L.; Yamada, E.; Swarup, K.; Nibau, C.; Bassel, G.; Choudhary, A.; et al. AtMYB93 is a novel negative regulator of lateral root development in *Arabidopsis*. *New Phytol.* **2014**, *4*, 1194–1207. [[CrossRef](#)]
52. Gibbs, D.; Coates, J. AtMYB₉₃ is an endodermis-specific transcriptional regulator of lateral root development in *Arabidopsis*. *Plant. Signal. Behav.* **2014**, *9*, e970406. [[CrossRef](#)] [[PubMed](#)]
53. Lev-Yadun, S.; Berleth, T. Expanding ecological and evolutionary insights from wild *Arabidopsis thaliana* accessions. *Plant. Signal. Behav.* **2009**, *4*, 796–797. [[CrossRef](#)]
54. Baxter, I.; Brazelton, J.N.; Yu, D.; Huang, Y.S.; Lahner, B.; Yakubova, E.; Li, Y.; Bergelson, J.; Borevitz, J.O.; Nordborg, M.; et al. A coastal cline in sodium accumulation in *Arabidopsis thaliana* is driven by natural variation of the sodium transporter AtHKT1;1. *PLoS Genet.* **2010**, *6*, e1001193. [[CrossRef](#)]
55. James, G.V.; Patel, V.; Nordström, K.J.; Klasen, J.R.; Salomé, P.A.; Weigel, D.; Schneeberger, K. User guide for mapping-by-sequencing in *Arabidopsis*. *Genome Biol.* **2013**, *14*, R61. [[CrossRef](#)]